Journal of Molecular Catalysis B: Enzymatic 69 (2011) 154–160

Contents lists available at ScienceDirect

Journal of Molecular Catalysis B: Enzymatic

journal homepage: www.elsevier.com/locate/molcatb

Sucrose hydrolysis by invertase immobilized on functionalized porous silicon

Mehrnoosh Azodi [a], Cavus Falamaki [a,*], Afshin Mohsenifar [b]

[a] Chem. Eng. Dept., Amirkabir University of Technology, 15875-4413, Tehran, Iran
[b] Department of Toxicology, Tarbiat Modares University, Tehran, Iran

ARTICLE INFO

Article history:
Received 6 October 2010
Received in revised form 24 January 2011
Accepted 24 January 2011
Available online 28 January 2011

Keywords:
Porous silicon
Invertase
Immobilization

ABSTRACT

A successful recipe for the production of immobilized invertase/porous silicon layer with appropriate catalytic behavior for the sucrose hydrolysis reaction is presented. The procedure is based on support surface chemical oxidation, silanization, activation with glutaraldehyde and finally covalent bonding of the free enzyme to the functionalized surface. The catalytic behavior of the composite layer as a function of pH, temperature, and the current density applied in the porous silicon (PS) preparation is investigated. Interestingly, V_{max} undergoes a substantial increase (ca. 30%) upon immobilization. The value of K_m increases by a factor of 1.53 upon immobilization. The initial activity is still preserved up to 28 days while the free enzyme undergoes a 26% loss of activity after the same period. Based on the outcomes of this study, we believe that tailored PS layers may be used for the development of new bioreactors in which the active enzyme is immobilized on the internal walls and is not lost during the process.

1. Introduction

Porous silicon (PS) is a very attractive candidate for the production of immobilized enzyme bioreactors. Relevant published reports are relatively still limited [1–10] but the future is promising. Enzymes like glucose-oxidase [2–4], ascorbate-oxidase [3], glucuronidase [5], gluthathion-s-transferase [6], urease [9,10], azurine and laccase [10] have been immobilized on PS so far. Studies on the development of biochemical process monitoring micro-systems based on PS have used microreactors consisting of etched micron-sized trench structures [1–4]. In other cases, plain thin films of PS have been subject of investigation [5–10].

The present work focuses on the immobilization of invertase (β-froctofuranosidase) on PS thin films. Invertase is industrially used for the production of glucose/fructose equimolar solutions by catalyzing the hydrolysis of sucrose. The latter product has a wide application in food industries, especially for the production of colorless, low crystallinity confectionary sweeteners: fructose syrups [11]. Due to the vast use of this enzyme in the food industries, several attempts have already been performed to immobilize it on different supports in order to extend its stability, providing re-usage possibility and preventing its loss upon processing. Many different supports have been investigated [11–18].

The immobilization process has been mostly realized by covalent bonding of the amino-groups of the protein to the proper functional groups of the support. Generally, invertase immobilization resulted in improved stability of the enzyme [13–18], while the enzyme–substrate affinity and/or enzyme–substrate complex intermediate to product "*transformation reaction rate constant*" reduced in most of the cases. The reported improved enzyme stability upon immobilization may be attributed to the occurrence of enzyme multipoint or multi-subunit attachment (preferably covalent) to the support [19,20]. Torres et al. [21] studied the stability of invertase immobilized by ionic adsorption on Sepabeads. Their work clearly shows that the state of oligomerization of the enzyme depends strongly on the solution pH. In addition, release of the enzyme subunits of the immobilized enzyme depends on the solution pH too. Therefore, it goes without saying that a successful immobilization of invertase is a tricky task. To the authors' knowledge this is the first study on the immobilization of invertase on PS.

Porous silicon is a versatile material in the sense that it can be produced in a wide range of porosity, pore size distribution, specific surface area and thicknesses. If produced through electrochemical etching, these properties may be tailored by choosing the appropriate controlling parameters (electrolyte composition, current density, time, etc.) [22].

PS has many advantages for being used as a support: (a) its microstructure can be tailored, (b) it provides large outermost surface, (c) its surface may be properly functionalized and (d) it is not subject to microbial attack. The structure of PS and the immobilization method embrace innumerable choices, thus probably providing the possibility of achieving an immobilized enzyme with desired properties.

This study presents a successful recipe for the production of immobilized invertase (from Candida utilis)/PS layer with appro-

* Corresponding author. Tel.: +98 21 64543160, fax: +98 21 66405847.
E-mail address: c.falamaki@aut.ac.ir (C. Falamaki).

1381-1177/$ – see front matter © 2011 Elsevier B.V. All rights reserved.
doi:10.1016/j.molcatb.2011.01.011

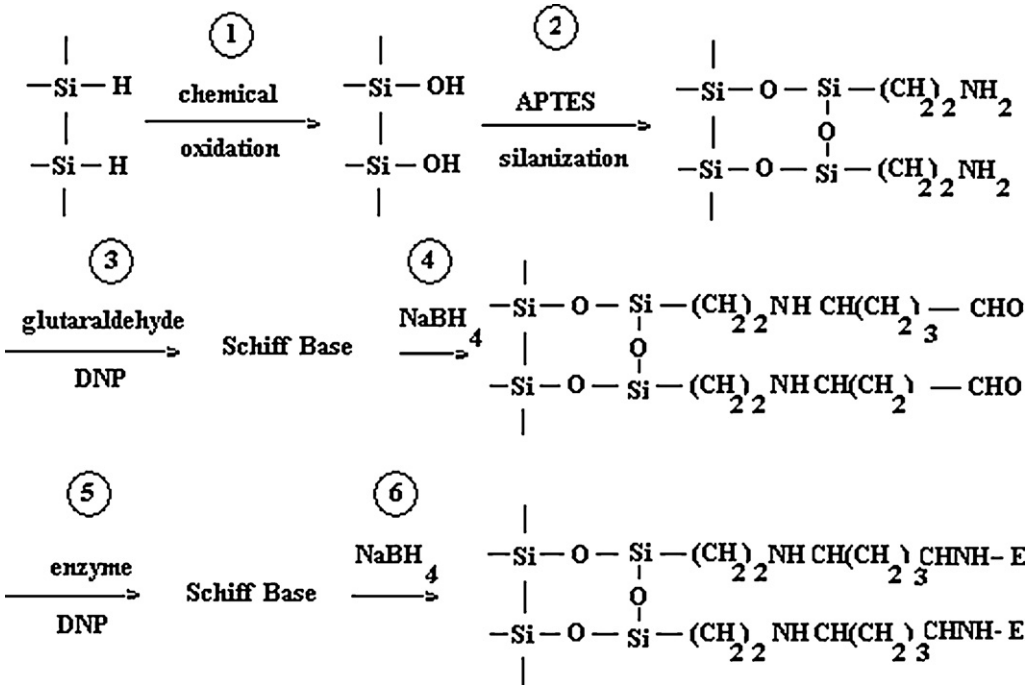

Fig. 1. Scheme of the PS layer functionalization and immobilization procedure.

priate catalytic behavior for the sucrose hydrolysis reaction. The general immobilization procedure adopted in this research comprehends the following steps: (a) PS fabrication by electrochemical etching, (b) chemical oxidation of surface, (c) silanization (with β-(triethoxysilyl)-propylamine), (d) activation with glutaraldehyde and (e) enzyme immobilization. Each step is followed by FT-IR spectroscopy to monitor the functionalization or enzyme immobilization steps. Glutaraldehyde activated supports have been reported to provide multipoint or multi-subunit immobilization of enzymes [23]. This is while the chemistry behind is still a matter of debate [24,25]. It will be shown that the glutaraldehyde route is successful in providing an immobilized enzyme with improved stability. The catalytic behavior of the composite layer as a function of pH, temperature, and the current density applied in the PS preparation is investigated. It should be noted that except the work of Maia et al. [8], published reports [1–7,9,10] on enzyme immobilization on PS did not investigate the pH and temperature dependency of the catalytic behavior and hence, did not obtain the optimum process conditions. The kinetic parameters K_m and V_m are determined and compared with their free enzyme counterparts. The effect of current density on the immobilized enzyme activity is also investigated.

2. Experimental

2.1. PS fabrication

Highly boron doped silicon wafers (0.002 and 0.01 Ω cm resistivity) were used throughout this study. Electrochemical etching was performed using a setup reported elsewhere [21]. Electrochemical etching was performed with a CVTM V1.00 galvanostat. Three current densities of 51, 76 and 127 mA cm^{-2} have been used. The composition of the electrolyte was 1:1 (v/v) (40 wt.% HF (BDH), 99.99 wt.% ethanol MERCK). Specific surface area, pore size distribution and pore volume determination of raw and modified PS layers were performed using an Autosorb-1 (Quanta Chrome) apparatus.

2.2. PS functionalization

Fig. 1 shows the general scheme used for the PS layer functionalization and immobilization steps. After electrochemical etching, the PS samples were washed with a 96 wt.% ethanol aqueous solution and immediately subjected to a chemical oxidation treatment based on the work reported by Liu et al. [26]. For this means, two solutions were prepared. Solution A consisted of a mixture of NH_3 solution (25 wt.%), deionized water and H_2O_2 (30 wt.% aqueous solution) with volume proportions 1:1:5. Solution B consisted of a mixture of HCl solution (32 wt.%), deionized water and H_2O_2 (30 wt.% aqueous solution) with volume proportions 1:1:6. All chemicals were reagent grade and purchased from MERCK. The compositions of the A and B solutions had been optimized as to obtain maximum surface density of Si–OH groups. First, the PS was treated with solution A at 80 °C for 80 s. The treated PS was then put into contact with solution B at 80 °C for 240 s. The obtained PS was washed with deionized water.

In continuation, the PS was subjected to a silanization process using reagent grade β-(triethoxysilyl)-propylamine (APTES) purchased from MERCK. The silanization process was performed a liquid phase route [27]. For the latter treatment, a 95 wt.% ethanol aqueous solution was prepared with a pH between 4.5 and 5.5 using acetic acid to which APTES was added (10 vol.%). After 10 min, 3 mL of the latter solution was added to a plastic container consisting of the oxidized PS. The latter was shaken for 24 h at RT with a Pars Azma apparatus with an agitation rate of 100 rpm. The treated PS was then rinsed with a 96 wt.% ethanol solution and dried in an oven at 110 °C for 30 min.

The final product was used immediately for the next step without rinsing. In the next step, the silanized surface was activated with glutaraldehyde (GA) (25 wt.%, MERCK) according to the following procedure: (a) an aqueous GA solution with known concentration (2.5 wt.%) was prepared; (b) di-nitro-pyridine (DNP) was dissolved separately in hot water (1 mg DNP per 1 mL water) and then added drop-wise to the solution obtained in (a) (4 mg DNP solution per 20 mg glutaraldehyde solution); (c) 3 mL of the final solution was transferred to the container containing the silanized PS and shaken

at RT for 20 min; (d) solid $NaBH_4$ (reagent grade, MERCK) was dissolved in the aqueous solution of the vessel containing the treated PS (4 mg $NaBH_4$ per 20 mg solution); (e) the whole assembly was shaken at RT for 70 min; (f) the treated PS was washed with plenty of water (15 times rinsing with 4 mL deionized water).

2.3. Immobilization of invertase on PS

The final wet PS was then used for the enzyme immobilization step. For this step, first 15 mg invertase (β-fructofuranosidase, EC 3.2.1.26, grade X, Candida utilis, SIGMA) were dissolved into 3 mL phosphate buffer (pH = 7). Each PS sample was then exposed to a solution containing 3 mL of buffer solution and 20 μL of the enzyme solution. DNP and $NaBH_4$ solutions were added as in the previous section. The container containing the PS and supernatant solution was then shaken at 0 °C for 1.5 h with an agitation rate of 100 rpm. The final product was washed with plenty of the buffer solution with predetermined pH. The samples were maintained in the buffer at 5 °C solution for the kinetic experiments.

2.4. Determination of enzyme activity

To determine the immobilized enzyme activity, 30 mL of a 50 mM sucrose (MERCK) aqueous solution buffered at pH = 4.5 (phosphate buffer) was put into contact with the enzyme-immobilized PS. For this means, the wetting liquid of the PS was sucked up with paper tissue and dried at RT prior to the addition of the substrate solution. After addition of the substrate solution, the vessel was shaken in an incubator (311DA Labnet) at the desired temperature (55 °C) for 20 min with an agitation rate of 100 rpm. Afterwards, the inhibitor solution (0.5 M Na_2CO_3, 200 μL per mL buffer solution) was added according to [23] and shaking was continued for 5 min. The concentration of glucose (equal to fructose) in the final solution was determined using an enzymatic colorimetric method using a Glucose PAP SL diagnosis kit (ELI diagnosis TECH). Absorbance measurements were performed using a spectrophotometer (CECIL CE7250 Bio Aquarius) at the wavelength of 500 nm. For obtaining the Lineweaver–Burk plot at the optimum pH and temperature, 1, 2, 3, 4 and 5 mM sucrose buffer solutions were used.

2.5. FT-IR and FESEM analysis

FT-IR measurements were performed using a NICOLET (Nexus B70 FT-IR) apparatus. Field emission scanning electron microscopy (FESEM) was performed using a S-4160 Hitachi instrument.

3. Result and discussion

3.1. FT-IR analysis

Fig. 2 shows the FT-IR spectrum of PS layers subject to different treatments using a wafer of 0.002 Ω cm resistivity, 76 mA cm^{-2} current density and 10 min electrochemical etching time. Considering the raw PS layer, the strong peaks in the wave number range of 2000–2300 cm^{-1} show that the outermost surface of the PS layer consist of SiH_x species. It is observed that after the chemical oxidation step, the intensity of the SiH_x peaks reduces. In addition, the relative intensity in the range of 2500–3700 cm^{-1} increases significantly. This phenomenon is attributed to the transformation of the $Si–H_x$ into Si–OH species, making the surface hydrophilic [26]. The FT-IR spectrum of the raw PS showed three peaks at 2845, 2930 and 2952 cm^{-1} which is attributed to adsorbed hydrocarbon species from air before measurement. These persist, although with some shift in the spectrum of the chemically oxidized PS layer (2850, 2916 and 2963 cm^{-1}). The peaks at 1625 cm^{-1} of the raw

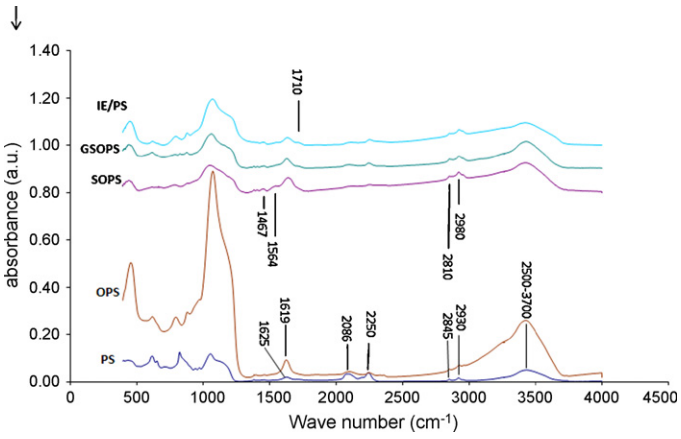

Fig. 2. FT-IR spectrum of PS layers subject to different treatments using a wafer of 0.002 Ω cm resistivity, 76 mA cm^{-2} current density and 10 min electrochemical etching time (PS = as synthesized PS, OPS = oxidized PS, SOPS = silanized OPS, GSOPS = SOPS reacted with glutaraldehyde, and IE/PS = immobilized enzyme on GSOPS composite layer).

PS and 1619 cm^{-1} of the treated PS are attributed to adsorbed water OH bending mode. Considering the oxidized PS treated with a 10 vol.% APTES solution, a new broad and high intensity zone comprehending many peaks appears after silanization in the range 1400–1650 cm^{-1}. The peaks at 1639 and 1564 cm^{-1} are attributed to the bending and scissor mode of NH bond, respectively. The peaks at 1467 and 1457 cm^{-1} are attributed to CH_x bonds. Before silanization, it is imperative to transform SiH_x entities into Si–OH ones. Accordingly, it is deduced that APTES resides on the PS outer surface. At this stage we cannot deduce the formation of covalent bonds between the Si atom of APTES molecule and the Si atom of PS on the outer surface (in the form of Si–OH). It is not possible to deduce the formation of new Si–O–Si bonds by considering the decrease of surface Si–OH groups due to the large IR adsorption of the OH groups of adsorbed water. Such a deduction has been reported previously by Liu et al. [26] but is scientifically not very robust. Also, a clear increase in the intensity of the peaks in the range 2810–2980 cm^{-1} due to CH_x bonds is observed. Recall that invertase is a carboxylic group rich acidic protein [17]. Considering the silanized PS layer treated with a 2.5 wt.% GA solution, the appearance of a distinct peak at 1710 cm^{-1} is attributed to the presence of carbonyl group of GA molecules. This might be a good sign showing that GA molecules did not react with all their carbonyl groups with the amine groups of the silanized PS, leaving free carbonyl groups for further reaction with the enzyme molecules. Comparing the FT-IR spectrum of the immobilized enzyme/PS (IE/PS) layer with the previous one, no observable change due to enzyme immobilization is observed. However, we cannot deduce the absence of the enzyme, as the latter sample showed high enzyme activity. The persistence of the 1710 cm^{-1} peak is attributed then to the carbonyl stretching vibration of the enzyme molecule. An important point is worth mentioning. Referring to Fig. 2, it is observed that SOPS (silanized–oxidized PS) contains a clear peak at 1564 cm^{-1}, which belongs to the free amine groups located on the exposed surface. Upon treatment with GA, the latter peak disappears (GSOPS curve in Fig. 2). This shows that the amine groups have been eliminated due to the eventual production of amide groups. Upon enzyme immobilization, if ionic adsorption of the enzyme molecules on the surface takes place, we should be able to observe the free amine groups of the enzyme in the FTIR spectrum of the final product as they do not convert to amide groups. However, it is clearly observed that the final product does not show any peak at 1564 cm^{-1} (or near it). Hence, any ionic adsorption of the enzyme, if existent, is scarce. Recall that we

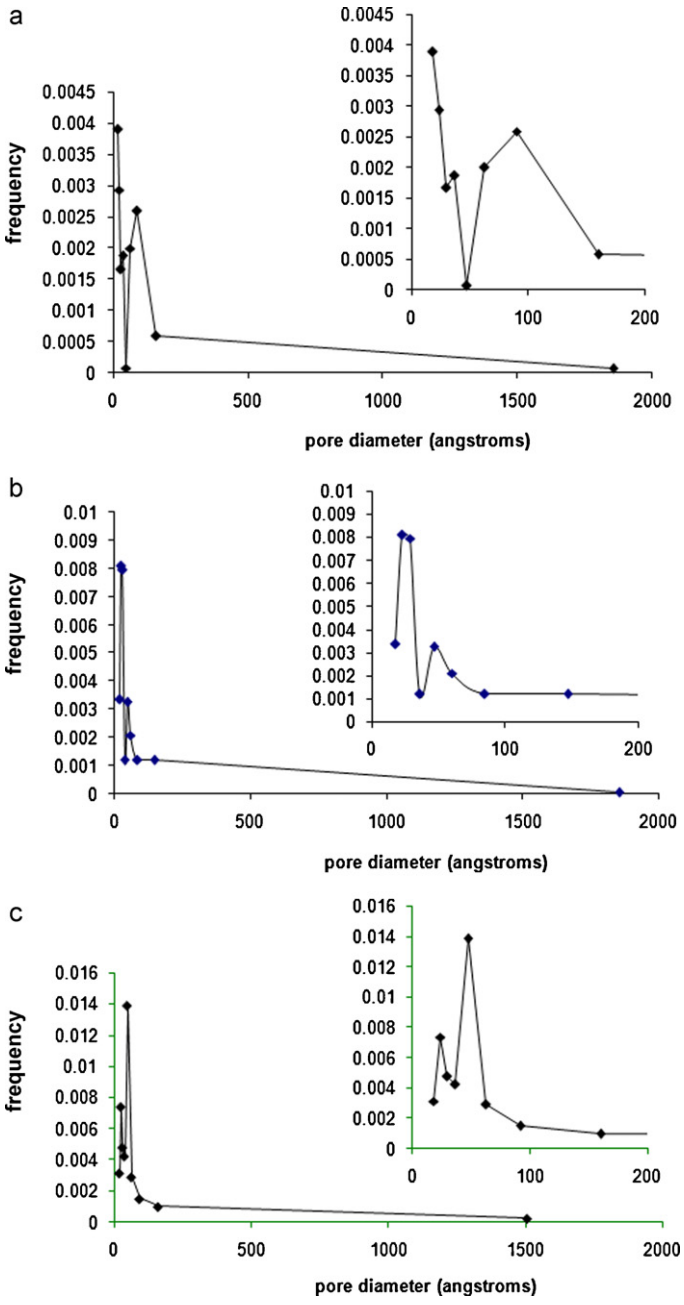

Fig. 3. (a) Pore size distribution of the IE/PS layer using a current density of 76 mA cm^{-2} and an etching time of 10 min based on the adsorption branch of the isotherm. (b) The same based on the desorption branch of the isotherm. (c) Pore size distribution of the PS layer after chemical oxidation using a current density of 76 mA cm^{-2} and an etching time of 10 min based on the adsorption branch of the isotherm.

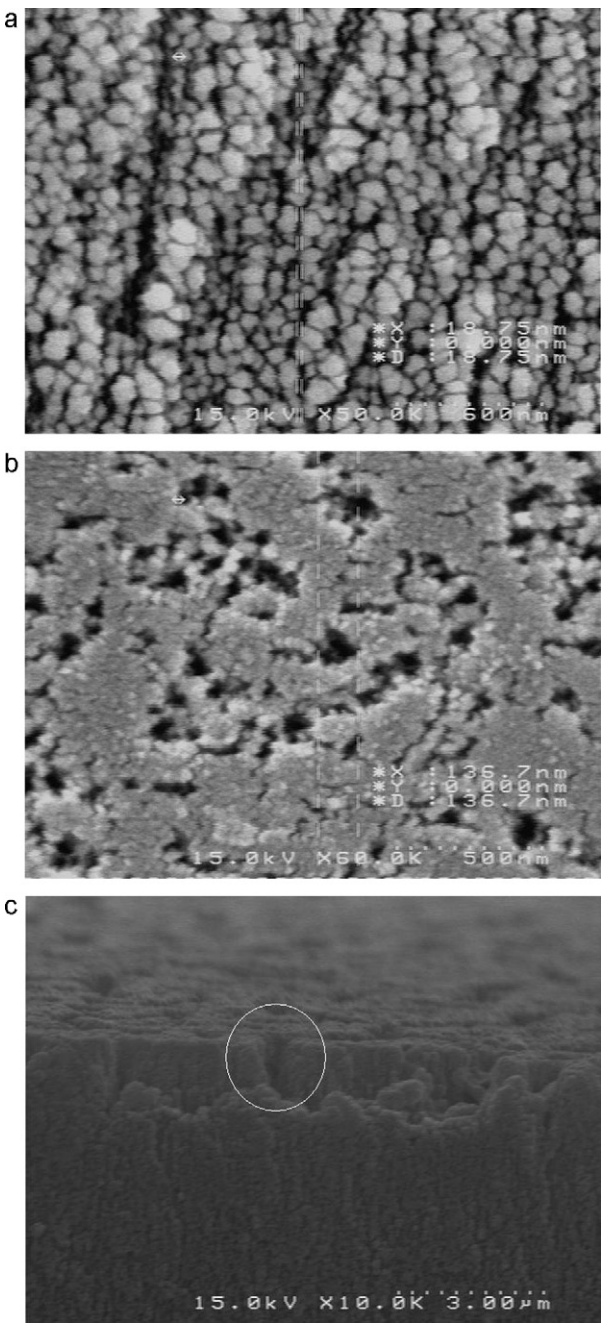

Fig. 4. FESEM pictures of the EI/PS layer (a) cross section, (b) top view and (c) both.

washed the final product several times with the buffer solution in order to exclude any 'adsorbed' species. By the way, if mere washing is not able to exclude adsorbed enzyme entities, the remaining molecules should be detectable by FTIR analysis, and this has not been the case.

3.2. Nitrogen adsorption and FESEM analysis

Fig. 3a and b shows the pore size distribution of the IE/PS layer using a current density of 76 mA cm^{-2} and an etching time of 10 min. The pore size distribution has been calculated based on the BJH (Braunauer, Emmett, Teller) methodology for the adsorption and desorption steps. The general trend resembles the one simulated by Tadvani and Falamaki [22] for boron-doped (1 0 0) Si wafers, but with a resistivity of 0.01 Ω cm. Both pore size distributions do possess three main peaks (1.9, 3.7 and 9.0 nm for the adsorption step and 2.2, 4.6 and 15 nm for the desorption step). The difference in the pore size distributions is due to the real shape and connectivity of the pores which do not obey exactly the main assumptions made in the BJH evaluation method. Based on the latter method, the average pore size is 5.1 nm for the adsorption and 4.9 nm for the desorption branches. An important point is the presence of a broad peak extending to sizes as large as 200 nm. Fig. 4a shows the corresponding FESEM picture of the cross-section of the EI/PS layer. Fig. 4b shows the surface of the PS layer under consideration. It is observed that large crater like pores with openings as large as 137 nm are present. Referring to Fig. 4c and considering the

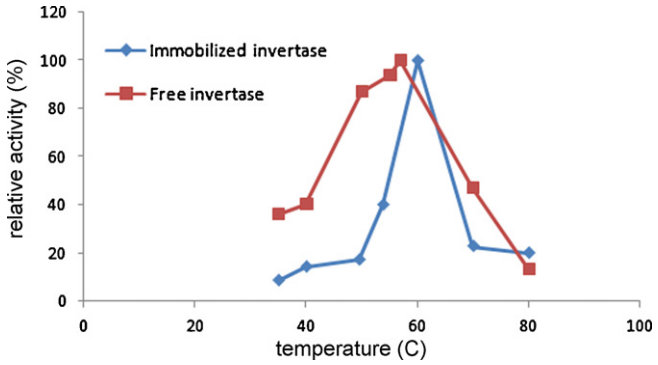

Fig. 5. The variation of the IE/PS and free enzyme activity versus temperature in the range of 35–80 °C.

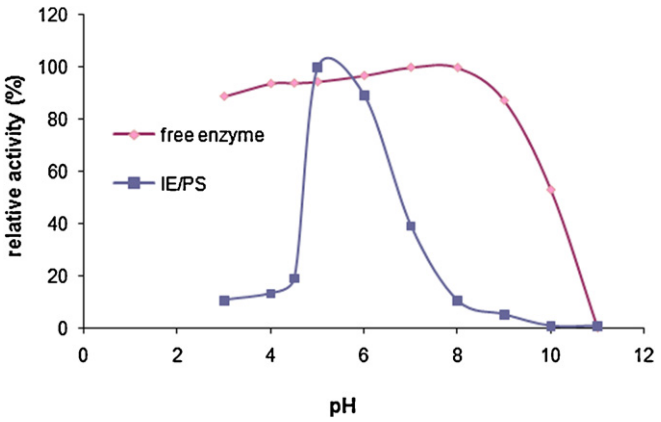

Fig. 6. pH dependency of the free enzyme and IE/PS activity.

indicated zone in the picture, it may be stated that the depth of the large surface pores might be as large as 1000 nm. This is in accordance with the results of the N_2 adsorption experiments. Such a non-uniformity of the pore-microstructure has also been reported for electrochemically etched n-type substrates by Letant et al. [5].

It is the opinion of the authors of this work that the main pores involved in the multi-step functionalization/enzyme immobilization process are those possessing a size larger than 20 nm. Such pores are scarce within the core of the PS layer, but constitute the majority of pores on the exposed surface of the PS layer. Theoretically, as shown by Tadvani and Falamaki [22], the pores initiated on the exposed surface of silicon upon electrochemical etching are usually at least one order of magnitude larger than the average pore size of the whole porous body. The SEM picture shown in Fig. 4b confirms the above explanation. Fig. 3c shows the pore size distribution of the PS layer under consideration just after the chemical oxidation step. Compared with Fig. 3a, it is observed that the pore size distribution remains approximately intact upon enzyme immobilization. This phenomenon can be explained considering the presence of large pores on the exposed surface of the PS layer.

3.3. Effect of temperature and pH on invertase activity

Most of the published reports on enzyme immobilization [11–18] referred to in Section 1 consider invertase enzyme from Saccharomyces cerevisiae yeast. The latter studies report an optimum pH in the range of 4–5 and an optimum temperature in the range of 45–60 °C for the enzyme activity.

The enzyme considered in this study is from Candida utilis yeast. Dickensheets et al. [28] reported an optimum pH for free invertase of Candida utilis equal to 4 and a range of 4–5.4 for the same immobilized on porous cellulose beads. Their work did not report an optimum temperature for the catalytic activity. On the other hand, Santana de Almeida et al. [29] report an optimum pH of 6 and optimum temperature of 70 °C for invertase obtained from Cladosporium cladosporiodes.

Based on the upper discussion, a pH of 4.5 was chosen for investigating the temperature dependency of the enzyme activity. The variation of the IE/PS and free enzyme activity versus temperature in the range of 35–80 °C is shown in Fig. 5. It is observed that a distinct optimum temperature of 57 °C exists. It is observed that the optimum temperature does not change significantly upon immobilization.

Accordingly, the optimum temperature was selected for investigating the pH dependency of the enzyme activity (Fig. 6). A pH range of 3–11 was chosen to study the optimum condition. It is observed that the optimum pH resides in the range of 7–8 for free invertase. It is observed that the trend of the curve changes abruptly upon immobilization. The optimum pH shifts from 7.5 to 5 and the curve narrows significantly. The curve is skewed towards the right showing that the IE/PS exhibits high activity in the span of pH equal to 5–6. The trend of the curve is significantly different from that reported in the literature [11–18,28].

The narrowing of the active ranges due to the immobilization process may be attributed mainly to conformation effects imposed by the support on the enzyme molecules.

3.4. Kinetic parameters

The kinetic parameters of the free and immobilized enzyme were determined by drawing the Lineweaver–Burk plot (Fig. 7) for the optimal parameters pH = 4.5 and reaction temperature of 57 °C. In both cases, a high correlation coefficient was obtained (>0.99), confirming the applicability of the Michaelis–Menten equation for the enzyme-catalyzed reaction. The values of K_m and V_{max} were calculated to be 0.0245 M and 0.944 mol min^{-1} for the free enzyme, respectively. The corresponding values of K_m and V_{max} for the immobilized enzyme were calculated to be 0.0376 M and 1.243 mol min^{-1}, respectively. The value of K_m increased by a factor of 1.53 upon immobilization. Published results on immobilized invertase report an increase of less than one order of magnitude for K_m in most of the cases [16,30,31]. We suppose that the decrease in the enzyme affinity versus the substrate upon immobilization is mainly due to eventual conformational changes. Substrate diffusion resistance is less pronounced as the immobilized enzymes do reside on the outermost and highly accessible surface of the PS, as discussed before.

An interesting result is the substantial increase (ca. 30%) of V_{max} upon immobilization. All published reports on invertase immobilization indicate a substantial decrease in V_{max}. In addition,

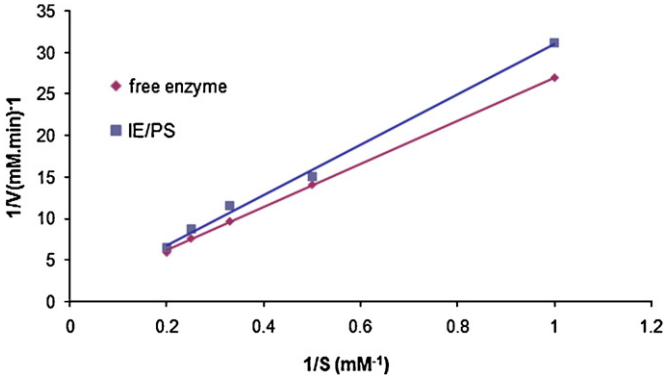

Fig. 7. Lineweaver–Burk plot for the free enzyme and IE/PS kinetic experiments.

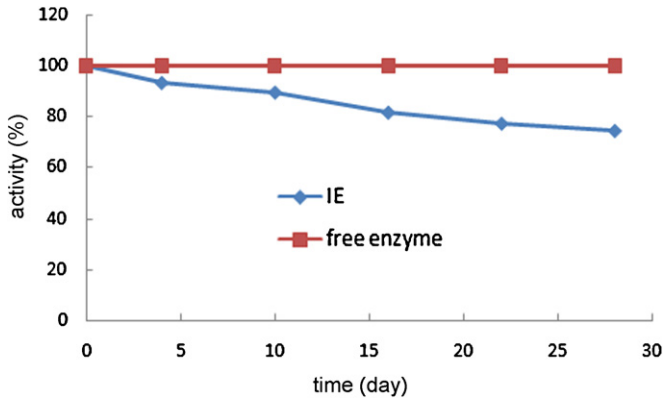

Fig. 8. The effect of storage time at 5 °C on the activity of free enzyme and IE/PS.

the few published investigations on enzyme immobilization on PS also show decrease in V_{max} (glutathione-s-transferase [6], β-glucuronidase [5]).

Reported values for V_{max} for free and immobilized enzymes other than invertase on PS show a sharp decrease (more than one order of magnitude) upon immobilization. The different behavior observed for the case of invertase immobilized on PS might be attributed to several phenomena like favorable change of enzyme structure upon immobilization and enhanced dissociation of the product from the product/enzyme complex. Another explanation may also hold: the raw enzyme may contain an industrial stabilizer. During the investigation of the free enzyme activity, the inhibitor leaves the enzyme dissolving into the buffer solution. However, it is not totally excluded from the system and may thus still induce a detrimental effect on the enzyme activity. Considering the immobilized enzyme, the inhibitor may be completely washed out during the 'cleaning process' through washing with plenty of the same buffer solution. In this case, the complete absence of the stabilizer may result in an increase of activity, i.e., a higher value of V_{max}.

Based on the difference between the activity of the enzyme in the solution of free enzyme and the same solution after being used for the immobilization on the functionalized PS support, an approximate value for the immobilization yield was calculated. The latter value is 91.7, 84.4 and 78.6% for the PS of 0.002 Ω cm resistivity for current densities 51, 76 and 127 mA cm^{-2}, respectively. The corresponding expressed activity has been 204.8, 185.1 and 53.6, respectively. The immobilization yield has been estimated to be 93.2, 86.3 and 51% for the PS of 0.01 Ω cm resistivity for current densities 51, 76 and 127 mA cm^{-2}, respectively. The corresponding expressed activity has been 133.8, 123.2 and 41.1 IU, respectively. It should be mentioned that the average standard deviation in the estimation of activity has been 16.7 IU.

3.5. Storage stability and reusability of IE

Fig. 8 shows the effect of storage time at 5 °C on the activity of IE. It is observed that initial activity is still preserved up to 28 days while the free enzyme undergoes a 26% loss of activity.

The reusability of the IE/PS was investigated for an operating pH and temperature of 5 and 60 °C, respectively. The initial activity was maintained intact up to the third treatment. After 7 treatments, the specific activity reduced to 33% of its original value.

3.6. Influence of current density of PS fabrication on enzyme activity

Fig. 9 shows the enzyme activity as a function of the current density of the electrochemical etching process for a pH of 5 and temperature of 60 °C. A significant increase in the activity (246%) is

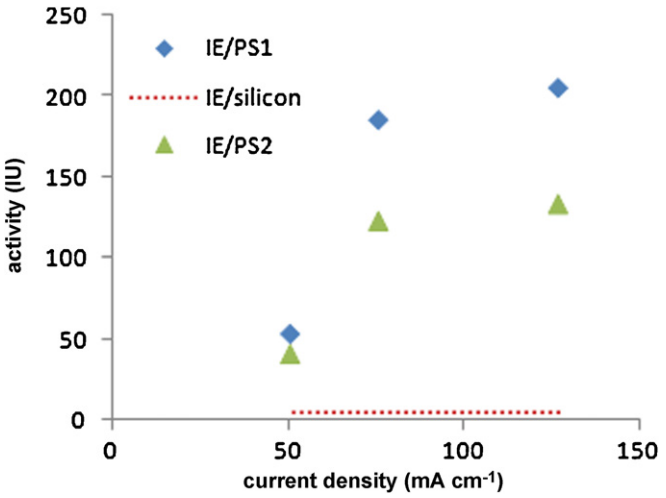

Fig. 9. Enzyme activity as a function of current density for a pH = 5 and temperature of 60 °C using etched wafer silicons of 0.002 Ω cm (IE/PS1) and 0.01 Ω cm (IE/PS2) resisistivity. The activity of the enzyme immobilized on not-etched silicon is also shown (0.002 Ω cm resistivity).

observed by increasing the current density from 51 to 76 mA cm^{-1}. Further increase of the current density to 127 mA cm^{-1} resulted in relatively slight increase in enzyme activity (11%). This phenomenon is attributed partly to the enlargement of the pores and more specifically, to the enlargement of the pores on the outermost PS layer [22]. The activity of the enzyme immobilized on plain silicon wafer (with the same geometrical exposed surface area) has been added for comparison. The same current density dependency of the IE/PS activity is observed when using a silicon wafer with a resistivity of 0.01 Ω cm and a similar preparation procedure as the chip with the resistivity of 0.002 Ω cm. However, the activity is generally less compared to the etched silicon wafer with the smaller resistivity of 0.002 Ω cm which may be simply attributed to a smaller pore size.

4. Conclusion

Invertase enzyme was immobilized successfully and for the first time on porous silicon. Although the affinity of the enzyme decreased upon immobilization (increase of K_m), the value of V_{max} increased significantly (30%).

The immobilization process enhances considerably the storage stability of the enzyme.

Based on the obtained experimental results, porous silicon may be considered a potential support for the industrial immobilization of invertase. The production of fructose syrup via sucrose hydrolysis is an important chemical process. Based on the outcomes of this study, we believe that tailored PS layers may be used for the development of new bioreactors in which the active enzyme is immobilized on the internal walls and is not lost during the process. Such reactors may then be used in a continuous mode.

References

[1] J. Drott, L. Rosengren, K. Lindstroem, T. Laurell, Thin solid films 330 (1998) 161–166.
[2] J. Drott, K. Lindstrom, L. Rosengran, T. Laurell, J. Micromech. Microeng. 7 (1997) 14–23.
[3] M. Bengtsson, S. Ekstrom, J. Drott, A. Collins, E. Csoregi, G. Marko-Varga, T. Laurell, Phys. Stat. Sol. 182 (2000) 495–504.
[4] M. Bengtsson, S. Ekstrom, G. Marko-Varga, T. Laurell, Talanta 56 (2002) 341–353.
[5] S.E. Letant, B.R. Hart, S.R. Kane, M.Z. Hadi, S.J. Shields, J.G. Reynolds, Adv. Mater. 16 (2004) 684–693.
[6] L.A. Delouise, B.L. Miller, Anal. Chem. 76 (2004) 6915–6920.

[7] L.A. Delouise, B.L. Miller, Anal. Chem. 77 (2005) 1950–1956.
[8] M.M.D. Maia, E.A. Vasconcelos, P.F.C.M.D. Maia, J.C. Maciel, K.R.R. Cajueiro, M.P.C. Silva, E.F. Silva, R.A.F. Dutra, V.N. Freire, J.L.L. Filho, Process Biochem. 42 (2007) 429–433.
[9] P.S. Chaudhari, A. Gokarna, M. Kulkarni, M.S. Karve, S.V. Bhoraskar, Sens. Actuators B 107 (2005) 258–263.
[10] A. Ressine, C. Vaz-Dominguez, V.M. Fernandez, A.L. De Lacey, T. Laurell, T. Ruzgas, S. Shleev, Biosens. Bioelectron. 25 (2010) 1001–1007.
[11] J.A. Santiago-Hernandez, J.M. Vasquez-Bahena, M.A. Calixto-Romo, G.B. Xoconostle-Cazares, J. Ortega-Lopez, R. Ruiz-Medrano, M.C. Montes-Horcasitas, M.E. Hidalgo-Lara, Enzyme Microb. Technol. 40 (2006) 172–176.
[12] Y. Chen, E.T. Kang, K.G. Neoh, K.L. Tan, Eur. Polym. J. 36 (2000) 2013–2095.
[13] A. Tanriseven, S. Dogan, Process Biochem. 36 (2001) 1081–1083.
[14] S. Akgol, Y. Kacar, A. Denizli, M.Y. Arica, Food Chem. 74 (2001) 281–288.
[15] T. Bahar, A. Tuncel, J. Appl. Polym. Sci. 83 (2002) 1268–1279.
[16] E. Sahmetlioglu, H. Yuruk, L. Toppare, I. Cianga, Y. Yagci, React. Funct. Polym. 66 (2006) 365–371.
[17] M.Y. Arica, G. Bayramoglu, J. Mol. Catal. B: Enzym. 38 (2006) 131–138.
[18] H. Altinok, S. Aksoy, H. Tumturk, N. Hasirci, J. Food Biochem. 32 (2008) 299–315.
[19] R. Fernandez-Laufente, Enzyme Microb. Technol. 45 (2009) 405–418.
[20] C. Mateo, J.M. Palomo, G. Fernandez-Lorente, J.M. Guisan, R. Fernandez-Laufente, Enzyme Microb. Technol. 40 (2007) 1451–1463.
[21] R. Torres, C. Mateo, M. Fuentes, J.M. Palomo, C. Ortiz, R. Fernandez-Laufente, J.M. Guisan, A. Tam, M. Daminati, Biotechnol. Prog. 18 (6) (2002) 1221–1226.
[22] J.K. Tadvani, C. Falamaki, Nanotechnology 19 (2008) 295701 (8 pp.).
[23] L. Betancor, F. Lopez-Gallego, A. Hidalgo, N. Alonso-Morales, G. Dellamora-Ortiz, C. Mateo, R. Fernandez-Laufente, J.M. Guisan, Enzyme Microb. Technol. 39 (2006) 877–882.
[24] Y. Wine, N. Cohen-Hadar, A. Freeman, F. Frolow, Biotechnol. Bioeng. 98 (2007) 711–718.
[25] I. Migneault, C. Dartiguenave, M.J. Bertand, K.C. Waldron, Biotechniques 37 (2004) 790–802.
[26] H.L. Liu, Y. Zhu, D. Xu, Y. Wan, L. Xia, X.S. Zhao, J. Appl. Phys. 105 (2009) 114307 (1–7).
[27] G.T. Hermanson, Bioconjugate Techniques, 2nd ed., Academic Press, 2008 (Chapter 13).
[28] P.A. Dickensheets, L.T. Chen, G.T. Tsao, Biotechnol. Bioeng. 19 (1977) 365–375.
[29] A.C. Santana de Almeida, L.C. de Araujo, A.M. Costa, C.A.M. de Abreu, A.G.M. de Andrade lima, M.L.A.P.F. Palha, Electron. J. Biotechnol. 8 (2005) 54–62.
[30] H. Tumturk, F. Arslan, A. Disli, Y. Tufan, Food Chem. 69 (2000) 5–9.
[31] T. Danisman, S. Tan, Y. Kacar, A. Ergene, Food Chem. 85 (2004) 461–466.